N91-19190

Progress in GaAs/$CuInSe_2$ Tandem Junction Solar Cells

N. P. Kim, R. M. Burgess, R. A. Mickelsen and B. J. Stanbery
Boeing Aerospace & Electronics
Seattle, WA

R. W. McClelland, B. D. King and R. P. Gale
Kopin Corporation
Taunton, MA

Introduction

Much more power is required for spacecraft of the future than current vehicles. To meet this increased demand for power while simultaneously meeting other requirements for launch, deployment, and maneuverability, the development of higher-efficiency, lighter-weight, and more radiation resistant photovoltaic cells is essential. Mechanically stacked tandem junction solar cells based on (AlGaAs)GaAs thin film CLEFT (Cleavage of Lateral Epitaxial Film for Transfer) top cells and $CuInSe_2$ (CIS) thin film bottom cells are being developed to meet these power needs.

The mechanically stacked tandem configuration is chosen due to its interconnect flexibility allowing more efficient array level performance. It also eliminates cell fabrication processing constraints associated with monolithically integrated multi-junction approaches [refs. 1-2], thus producing higher cell fabrication yields. The GaAs cell is used as the top cell due to its demonstrated high efficiency [ref. 3], and good radiation resistance [ref. 4]. Furthermore, it offers a future potential for bandgap tuning using AlGaAs as the absorber to maximize cell performance [ref. 5]. The $CuInSe_2$ cell is used as the bottom cell due to superb radiation resistance [ref. 4], stability, and optimal bandgap value in combination with an AlGaAs top cell. Since both cells are incorporated as thin films, this approach provides a potential for very high specific power. This high specific power (W/kg), combined with high power density (W/m^2) resulting from the high efficiency of this approach, makes these cells ideally suited for various space applications.

Cell Fabrication and Characterization

The schematic of the (AlGaAs)GaAs/$CuInSe_2$ tandem cells is shown in Figure 1. It consisted of a double-heterostructure (AlGaAs)GaAs CLEFT thin-film top cell and a polycrystalline $CuInSe_2$ thin-film heterojunction lower cell. All tandem cells were fabricated with a 4 cm^2 cell design.

The bottom $CuInSe_2$ cell was fabricated on a glass substrate whose thermal expansion coefficient is the same as or very similar to that of a coverglass. Fabrication of the CIS cell included sequential deposition of Mo back electrode, $CuInSe_2$ absorber

layer, and CdZnS window layer, and photolithographic patterning followed by etching to form a solar cell device. Grid metal deposition and anti-reflection coating were added to complete fabrication of the n-on-p CIS cell. A schematic of this cell is shown in Figure 2 and details of the fabrication process are found in prior publications [refs. 6-8]. Contact pads used for the interconnect of the top cell electrodes and the subarray string were formed during the lower cell fabrication when the contact pads for the lower cell electrode were formed.

The top (AlGaAs)GaAs thin-film cell was fabricated by the CLEFT process described elsewhere [refs. 9-10]. The schematic of the cell and the fabrication process are shown in Figure 3. A thin film layer was grown on a bulk GaAs substrate through seed lines using a vapor phase epitaxy method. The double-heterostructure n-on-p cell was formed by sequential growth of p-GaAs buffer, p+-AlGaAs BSF, p-GaAS base, n-GaAs emitter, n+-AlGaAs window and n+-GaAs cap layer. Further details on growth parameters are found in other publications [refs.10-11]. The thin-film was cleaved from the substrate after front grid metallization and support mounting. The structure was bonded to the $CuInSe_2$ cell using a space qualified adhesive after a gridded back metallization and transmission enhancement coating were applied. A single layer of SiN was normally used as the front side anti-reflection coating, although a double layer of SiN/Al_2O_3 was used on some cells to enhance light transmission to the bottom cell.

Interconnection from the top cell bonding pads to substrate bonding pads was made using a gold ribbon. A MgF_2 coated coverglass was mounted on the top of the tandem stack using a space qualified optically transparent adhesive.

Electrical measurements were conducted in the four terminal configuration at one sun and 28°C with an AM0 power normalization of 137.2 mW/cm^2. The GaAs I-V characteristics were measured at Kopin. An ORC 1000 solar simulator was used with a NASA calibrated AM0 GaAs reference cell. These measurements were found to be in good agreement with SERI and NASA measurements. The $CuInSe_2$ I-V characteristics were measured at Boeing using an AM0 filter-equiped Spectrolab XT-10 simulator. A JPL balloon flight calibrated solar cell consisting of a $CuInSe_2$ solar cell under an intimately contacted GaAs filter was used as the reference cell. Some GaAs cells were also measured at Boeing using the XT-10 simulator and adjusted following the procedure of the spectral mismatch calculation described elsewhere [ref.12]. The results also showed good agreement with Kopin's measurements. Some tandem cells were measured at Boeing using a recently acquired JPL balloon flight $GaAs/CuInSe_2$ tandem cell as the reference cell. When the same cells were measured at NASA, good agreement was also achieved.

Experimental Results

Cell Efficiency and Cell Weight

The best performance result achieved so far with 4 cm^2 tandem cells was 23.1% one sun AM0. This is the highest efficiency ever-reported for a thin film photovoltaic cell.

The I-V characteristics of this cell are shown in Figure 4. The subcell efficiencies of 20.6% and 2.5% were achieved for the GaAs top and the CIS bottom cells respectively, when the cell was measured at NASA Lewis Research Center. (The NASA measurements were conducted by Dr. D.J. Brinker.) Also included in the figure are the results of Boeing measurements that are indicated in the parentheses. This confirmed good agreement between the measurents by the two laboratories. The external spectral response curves of the same cell are shown in Figure 5 and indicate a significant improvement in IR response over the previously reported results [ref.7].

Among the completed tandem cells, the highest efficiency for the GaAs CLEFT cell was 20.6%. The highest efficiency for the $CuInSe_2$ cell under the GaAs CLEFT cell was improved to 3.0% using a double layer front AR coating on the GaAs CLEFT cell. The I-V characteristics and the external spectral response curves are shown in Figure 6. These cells demonstrate that a total efficiency over 23.5% can be readily achieved using this approach without significant process or structure changes. Further improvement up to 26% is projected when AlGaAs is incorporated as the absorber in the top cell.

Among the 4 cm^2 tandem cells on 2-mil glass, the highest efficiency achieved thus far was 20.8% one sun AM0. The subcell efficiencies of 18.2% and 2.6% were measured for the GaAs top and the $CuInSe_2$ bottom cells respectively. The I-V characteristics and the external spectral response curves of this cell are shown in Figure 7 and Figure 8. This cell weighed 188 mg without optimal substrate trimming before coverglass mounting, and provided a cell power output of 113 mW. After mounting a 1-mil thick coverglass using a space qualified adhesive, the cell weighed 258 mg, and provided an power ouput of 114 mW, yielding a cell-coverglass specific power of 442 W/kg. Cell-coverglass specific power up to 630 W/kg is projected with a 2-mil thick coverglass when optimal substrate and adhesive thicknesses are incorporated. Further improvement in specific power up to 750 W/kg is expected when the projected efficiency of 26% is achieved.

Environmental Effects

The radiation resistance of this tandem cell structure is expected to be excellent. Results of radiation experiments conducted with bare cells confirmed that the $CuInSe_2$ cells have superior radiation resistance compared to Si or GaAs cells, and that the

thin-film double-heterostructure GaAs cells are as resistant as bulk GaAs cells to 1 MeV protons and more resistant to 0.2 MeV protons and 1 MeV electrons. Details of this experiment have been reported elsewhere [ref.4].

An experiment was conducted to confirm the stability of the $CuInSe_2$ cell in a vacuum environment. The experiment consisted of exposure of the $CuInSe_2$ cells to pressure as low as 1×10^{-7} torr at various temperatures from 25°C to 110°C. No cell performance degradation was observed during this experiment. A thermal cycling experiment was also conducted to confirm survivability of tandem cell structure and ribbon interconnects by subjecting interconnected 4 cm^2 tandem cells to thermal cycling from 80°C to −130°C for up to 850 cycles. No significant difference in electrical characteristics was observed between the experimental samples and the control samples stored at room temperature.

Potential Applications

A voltage-matched module circuit based on three GaAs cells in parallel and three $CuInSe_2$ cells in series is proposed as a possible circuit unit. The schematic of this module string is shown in Figure 9. Even though this highly automatable interconnect method is sufficiently flexible to permit any circuit configuration, the present approach is based on a voltage-matched string. Since the temperature dependence of the tandem cell power and voltage at maximum power are important parameters for array and power system design, the temperature dependence of this tandem cell was characterized and the results plotted in Figure 10. As the $CuInSe_2$ cell power output is much less sensitive to voltage in the neighborhood of the maximum power point voltage, this voltage-matched two terminal configuration achieves over 98% of the four terminal circuit output over a broad operating temperature range as shown in Figure 11.

Correlation of on-orbit array level circuit performance in space to cell performance at the standard test conditions in the labaratory is complex, especially for the tandem cell, and difficult due to the application-specific nature of array performance optimization methods. Three generic orbits were chosen with two array structures, rigid and flexible, to compare the impacts of different cell technologies on the array level performance. Optimization of shielding thickness was conducted to minimize the array weight for the fixed end-of-life power output. Data available in the literature (refs. 4 and 13) were used for calculation of radiation and temperature effects on cell performance. The advanced photovoltaic solar array (APSA) design developed for JPL [ref. 14] was used as the base for the flexible array in the analysis. As shown in Table 1 and Table 2, this tandem cell approach provides significant array level weight and area savings over other cell technologies.

Program Status

We have recently increased our tandem cell throughput and fabricated quantities of cells that produce tens of watts of power in total. A significant increase in cell throughput and a 2 cm x 4 cm cell design with high active area utilization, and further performance improvement using AlGaAs instead of GaAs as absorber are currently being investigated to make GaAs(AlGaAs)/$CuInSe_2$ tandem cells more viable for near-term space power applications.

Conclusions

The efficiency of GaAs/$CuInSe_2$ thin-film tandem cells improved to 23.1%, one sun, AM0. This is the highest efficiency ever-reported for a thin-film photovoltaic cell. Further improvement up to 26% is projected when an AlGaAs absorber layer is incorporated in the top cell.

Lightweight GaAs/$CuInSe_2$ tandem cells (2-mil thick) were demonstrated with efficiencies as high as 20.8%. The cell with a 1-mil thick coverglass weighed 258 mg even without optimal substrate trimming. This provides a cell-coverglass specific power of 442 W/kg, and offers a potential for specific powers up to 750 W/kg with an AlGaAs top cell.

Environmental tests including radiation test, vacuum experiment and thermal cycling test were conducted and provided favorable results. On-array level performance was analyzed for three generic orbit levels to compare the impact of different cell technologies, and results indicated that a significant array weight and area savings can be achieved with these tandem cells. A voltage-matched module circuit is proposed and its projected performance is discussed. The current status of the program and the near term plan is also summarized.

References

[1.] H. F. MacMillan, H. C. Hamaker, G. F. Virshup and J. G. Werthen, *Conference Record 20th IEEE Photovoltaic Specialist Conference*, 48, 1988.

[2.] S. P. Tobin, S. M. Vernon, C. Bajgar, V. E. Haven, L. M. Geoffroy, M. M. Sanfacon, D. R. Lillington, R. E. Hart, K. A. Emery and R. J. Matson, *Conference Record 20th IEEE Photovoltaic Specialist Conference*, 405, 1988.

[3.] N. Ogasawara, S. Ochi, N. Hayafuji, M. Kado, K. Mitsui, K. Yamanaka, and T. Murotani, *Technical Digest of the International PVSEC-3*, 477, Tokyo, Japan, 1987.

[4.] R. M. Burgess, W. S. Chen, W. E. Devaney, D. H. Doyle, N. P. Kim, and B. J. Stanbery, *Conference Record 20th IEEE Photovoltaic Specialist Conference*, 909, 1988.

[5.] J. C. C. Fan and B. J. Palm, Solar Cells **12**, 401, 1984.

[6.] B. J. Stanbery, J. E. Avery, R. M. Burgess, W. S. Chen, W. E. Devaney, D. H. Doyle, R. A. Mickelsen, R. W. McClelland, B. D. King, R. P. Gale and J. C. C. Fan, *Conference Record 19th IEEE Photovoltaic Specialist Conference*, 280,1987.

[7.] N. P. Kim, R. M. Burgess, B. J. Stanbery, R. A. Mickelsen, J. E. Avery, R. W. McClelland, B. D. King, M. J. Boden and R. P. Gale, *Conference Record 20th IEEE Photovoltaic Specialist Conference*, 457, 1988.

[8.] R. A. Mickelsen, and W. S. Chen, *Conference Record 16th IEEE Photovoltaic Specialist Conference*, 781, 1982.

[9.] R. W.McClelland, C. O. Bozler and J. C. C. Fan, Appl. Phys. Lett. **37**, 560, 1980.

[10.] R. P. Gale, R. W. McClelland, B. D. King and J. V. Gormley, *Conference Record 20th IEEE Photovoltaic Specialist Conference*, 446, 1988.

[11.] R. P. Gale, J. C. C. Fan, G. W. Turner, and R. L. Chapman, *Conference Record 18th IEEE Photovoltaic Specialist Conference*, 296, 1985.

[12.] K. A. Emery, C. R. Osterwald, T. W. Cannon, D. R. Myers, J. Burdick, T. Glastfelter, W. Czubatyj and J. Yang, *Conference Record 20th IEEE Photovoltaic Specialist Conference*, 1246, 1988.

[13.] C. R. Osterwald, T. Glatfelter, and J. Burdick, *Conference Record 19th IEEE Photovoltaic Specialist Conference*, 188, 1987.

[14.] R. M. Kurland and P. Stella, *Proceedings of 9th Space Photovoltaic Research and Technology Conference*, 122, 1988, and also see *Advanced Photovoltaic Solar Array Prototype Fabrication*, Final Review Data Package, TRW Report No. 51760-6002-UT-00, JPL Contract No. 957990.

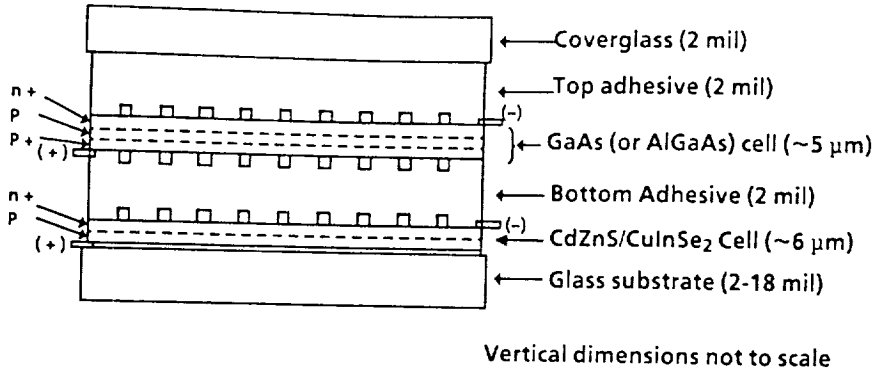

Figure 1. Schematic of Tandem Cell Structure

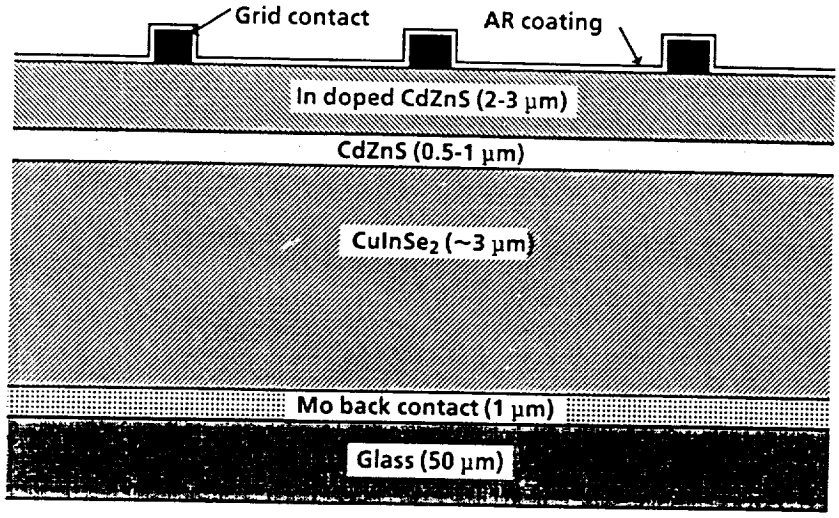

Figure 2. Cross Sectional View of $CuInSe_2$ Cell

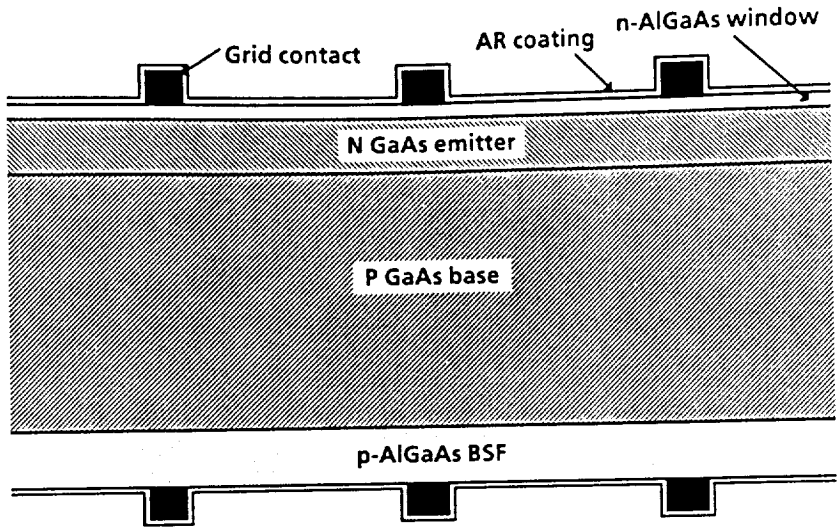

(a) Cross Sectional View of GaAs Thin-film Cell

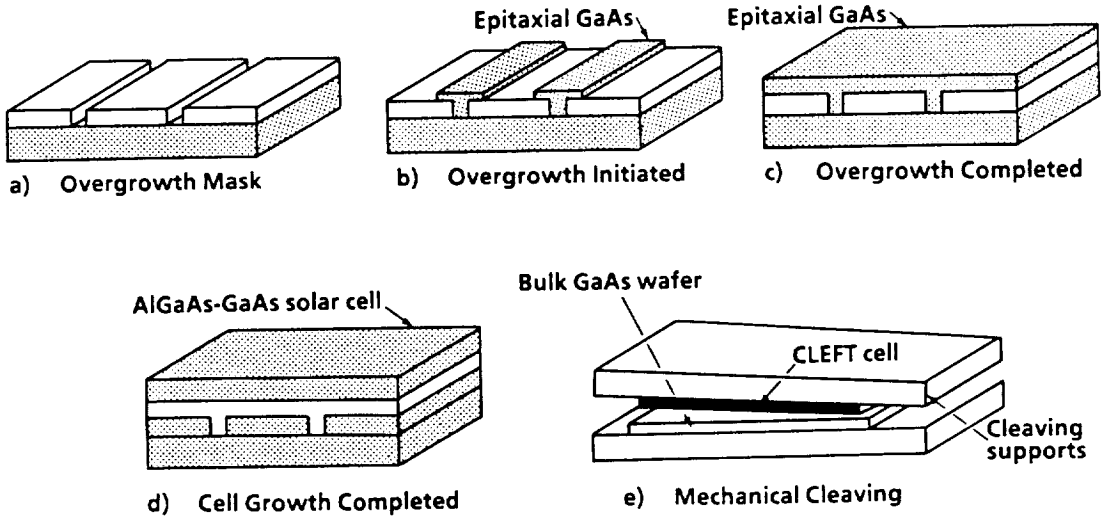

(b) Sequence of GaAs CLEFT Process (Solar cell device processing steps are not included)

Figure 3. Structure and Process Sequence of GaAs CLEFT Cell

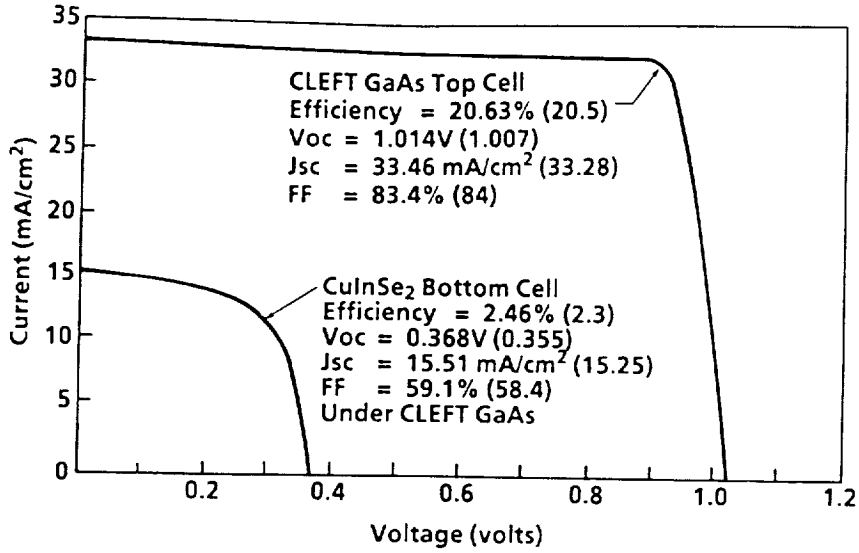

( ) Boeing measurements

- Total efficiency: 23.1% (22.8)
- Cell area: 4 cm^2

Figure 4. I-V Data on NASA Measured GaAs/$CuInSe_2$ Tandem Cell

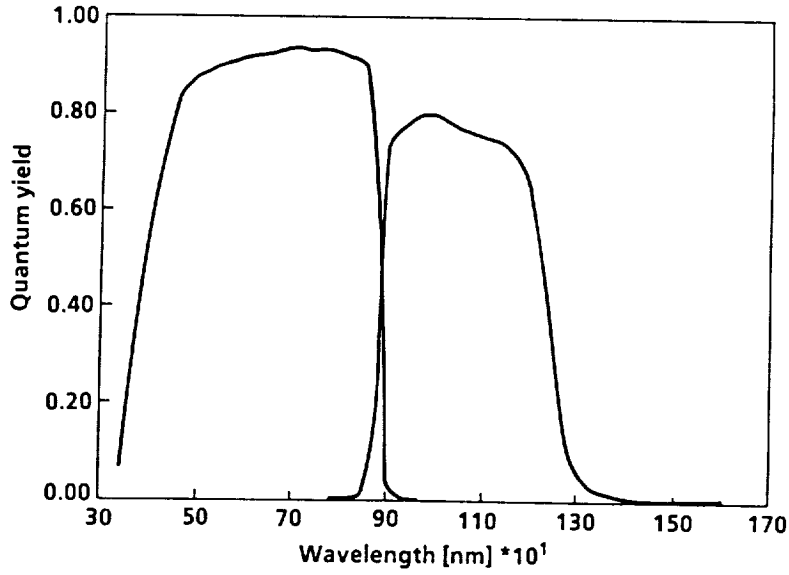

Figure 5. Spectral Response of A Tandem Cell

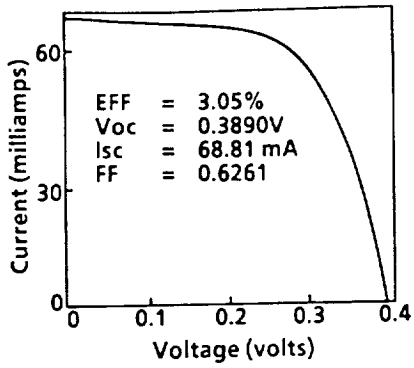

a) I-V Curves From a $CuInSe_2$ Cell Under the GaAs CLEFT

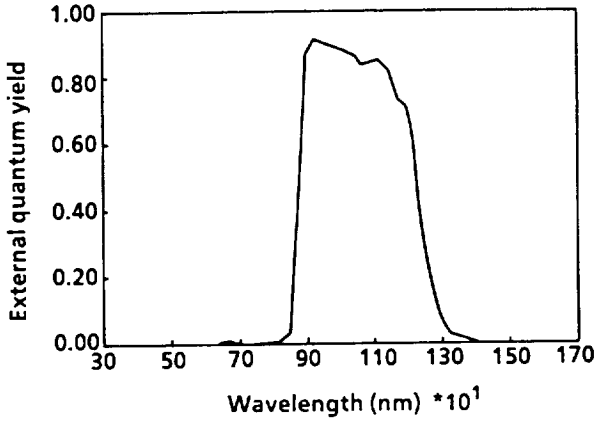

b) Spectral Response Curves From a $CuInSe_2$ Under the GaAs CLEFT

Figure 6. I-V and Spectral Response Curves From a $CuInSe_2$ Cell under the GaAs CLEFT Cell

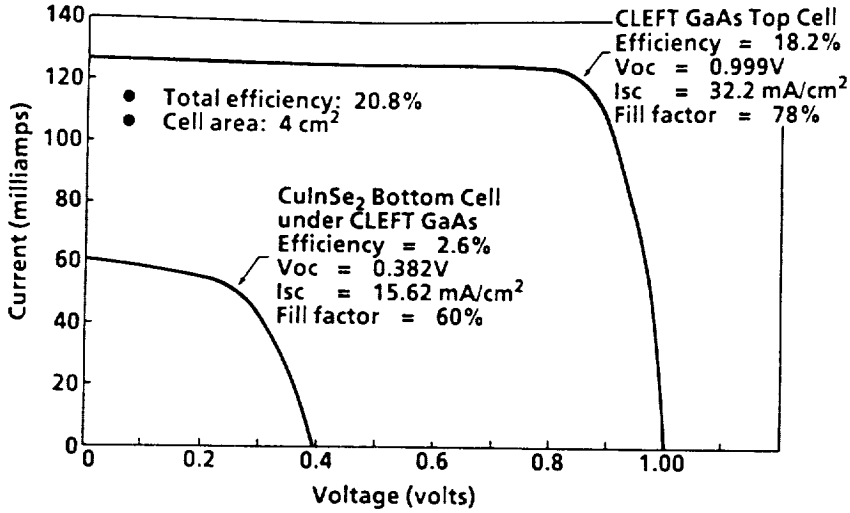

Figure 7. I-V Curves From a Lightweight Tandem Cell on 2-mil Substrate

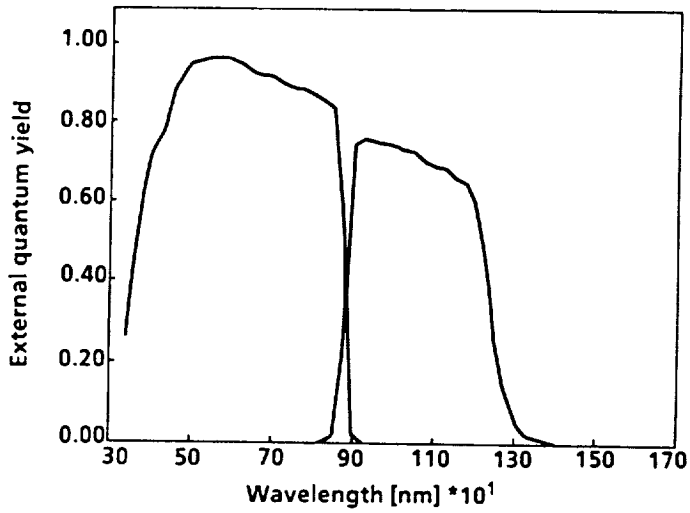

Figure 8. Spectral Response Curves From a Lightweight Tandem Cell on 2-mil Substrate

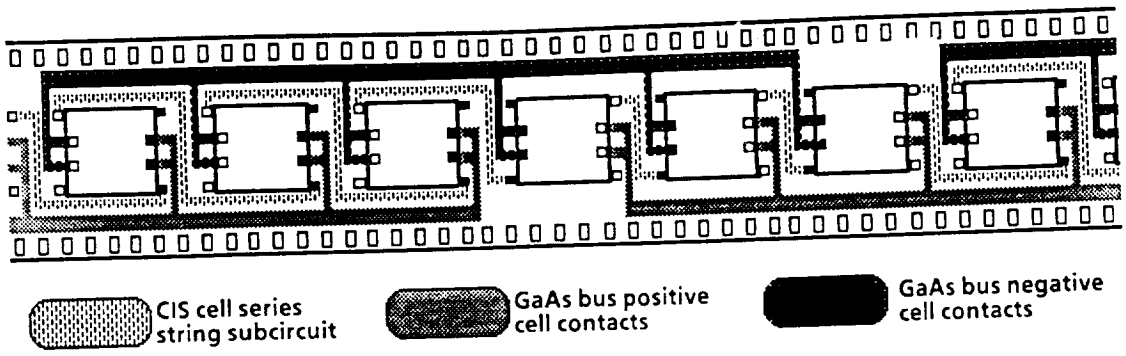

Figure 9. Schematic of Buss Interconnection for a Voltage-Matched String (The figure is not meant to illustrate the actual conductor pattern layout.)

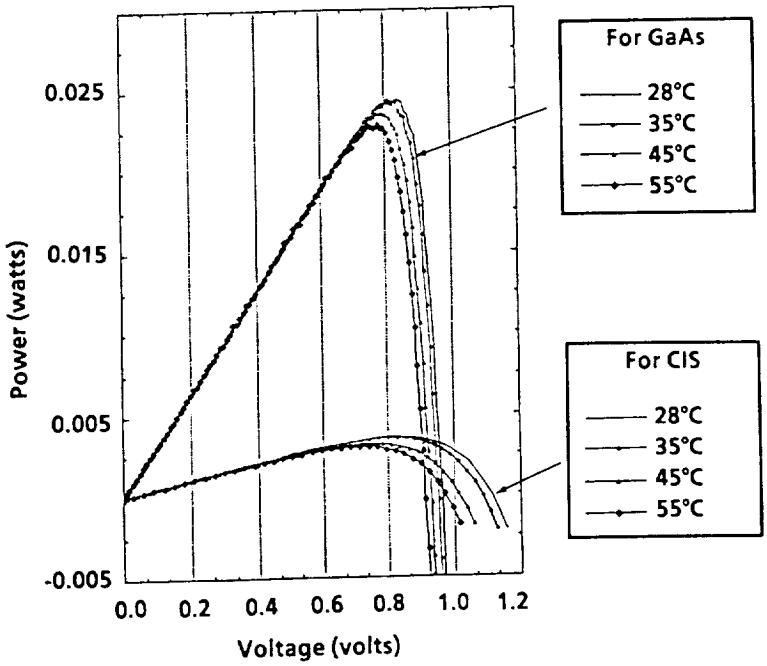

Figure 10. Power vs. Voltage Curves At Various Temperatures (Four terminal measurement, Plotted CIS voltages are three times of the actual CIS voltages.)

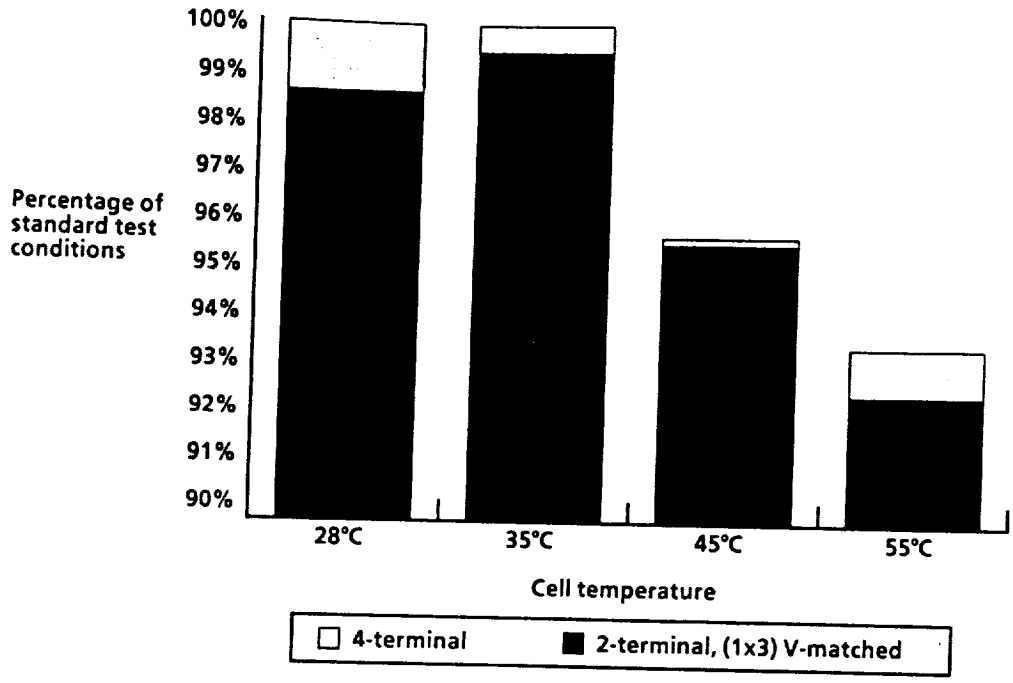

Figure 11. Relative Performance of a Voltage-Matched Two-Terminal String

Cell Technology (Thickness, BOL Efficiency at 28° C) / Orbital Environment	Silicon (8 mil, 14%)		Silicon (2 mil, 13.5%)		GaAs (8 mil, 19%)		GaAs/Ge (3 mil, 19%)		CLEFT GaAs (Thin, 2 mil substrate, 19%)		CLEFT GaAs/CIS Tandem (Thin, 2 mil substrate, 22%)	
	Array Weight (Kg)	Array Area (m^2)	Array Weight (Kg)	Array Area (m^2)	Array Weight (Kg)	Array Area (m^2)	Array Weight (Kg)	Array Area (m^2)	Array Weight (Kg)	Array Area (m^2)	Array Weight (Kg)	Array Area (m^2)
Low-Earth Orbit (LEO) • 270 N.M. Circular, 53° inclination • 5 year lifetime	89	19	78	18	182	13	65	14	60	13	53	12
Optional shielding thickness	All cases contain minimum shieldings of 2 mil thick coverglass and 5 mil thick Al facesheets											
Mid-Earth Orbit (MEO) • 5700 N.M., circular, 63° inclinaton • 7 year lifetime	157	24	147	24	229	15	100	17	102	16	85	16
Optional shielding thickness	F:27 mil, B:19 mil		F:25 mil, B:22 mil		F:27 mil, B:10 mil		F:22 mil, B:10 mil		F:22 mil, B:22 mil		F:18 mil, B:10 mil	
Geosynchronous Earth Orbit (GEO) • 19,700 N.M., circular, 0° inclination • 10 year lifetime	95	21	82	20	191	14	68	15	62	14	55	12
Optional shielding thickness	All cases contain minimum shieldings of 2 mil thick coverglass and 5 mil thick Al facesheets											

Table 1. Array Level Performance Comparison (For 2.5 KW EOL Rigid Array)

Cell Technology (Thickness, BOL Efficiency at 28° C) / Orbital environment	Silicon (4 mil, 14%)		Silicon (2 mil, 13.5%)		GaAs/Ge (3 mil, 19%)		CLEFT GaAs (Thin, 2 mil substrate, 19%)		CLEFT GaAs/CIS Tandem (Thin, 2 mil substrate, 22%)	
	Array Weight (Kg)	Array Area (m^2)	Array Weight (Kg)	Array Area (m^2)	Array Weight (Kg)	Array Area (m^2)	Array Weight (Kg)	Array Area (m^2)	Array Weight (Kg)	Array Area (m^2)
Low-Earth Orbit (LEO) • 270 N.M. Circular, 53° inclination • 5 year lifetime	47	41	41	39	41	30	35	27	34	25
Optional shielding thickness	All cases contain minimum shielding of 2 mil thick coverglass									
Mid-Earth Orbit (MEO) • 5700 N.M., circular, 63° inclinaton • 7 year lifetime	188	60	186	59	112	42	112	39	95	37
Optional shielding thickness	F:22 mil, B:20 mil		F:21 mil, B:20 mil		F:18 mil, B:10 mil		F:18 mil, B:4 mil		F:17 mil, B:12 mil	
Geosynchronous Earth Orbit (GEO) • 19,700 N.M., circular, 0° inclination • 10 year lifetime	56	53	48	51	43	31	36	29	35	27
Optional shielding thickness	All cases contain minimum shielding of 2 mil thick coverglass									

Table 2. Array Level Performance Comparison (For 5 KW EDL Flexible Array)